Renin inhibition by substituted piperidines: a novel paradigm for the inhibition of monomeric aspartic proteinases?

C Oefner, A Binggeli, V Breu, D Bur, J-P Clozel*, A D'Arcy, A Dorn, W Fischli*, F Grüninger, R Güller†, G Hirth, HP Märki, S Mathews, M Müller, RG Ridley, H Stadler, E Vieira, M Wilhelm, FK Winkler and W Wostl

Background: The aspartic proteinase renin catalyses the first and rate-limiting step in the conversion of angiotensinogen to the hormone angiotensin II, and therefore plays an important physiological role in the regulation of blood pressure. Numerous potent peptidomimetic inhibitors of this important drug target have been developed, but none of these compounds have progressed past clinical phase II trials. Limited oral bioavailability or excessive production costs have prevented these inhibitors from becoming new antihypertensive drugs. We were interested in developing new nonpeptidomimetic renin inhibitors.

Results: High-throughput screening of the Roche compound library identified a simple 3,4-disubstituted piperidine lead compound. We determined the crystal structures of recombinant human renin complexed with two representatives of this new class. Binding of these substituted piperidine derivatives is accompanied by major induced-fit adaptations around the enzyme's active site.

Conclusions: The efficient optimisation of the piperidine inhibitors was facilitated by structural analysis of the renin active site in two renin–inhibitor complexes (some of the piperidine derivatives have picomolar affinities for renin). These structural changes provide the basis for a novel paradigm for inhibition of monomeric aspartic proteinases.

Address: Pharma Research Departments, F. Hoffmann-La Roche Ltd, CH-4070 Basel, Switzerland.

Present addresses: *Actelion Ltd, Gewerbestraße 16, CH-4123 Allschwil, Switzerland. †Chemspeed Ltd, Rheinstraße 32, CH-4302 Augst, Switzerland.

Correspondence: C Oefner or HP Märki
E-mail: christian.oefner@roche.com or hans_p.maerki@roche.com

Key words: aspartic proteinase, drug design, induced fit, renin, X-ray analysis

Received: **12 November 1998**
Revisions requested: **1 December 1998**
Revisions received: **9 December 1998**
Accepted: **16 December 1998**

Published: **11 February 1999**

Chemistry & Biology March 1999, **6**:127–131
http://biomednet.com/elecref/1074552100600127

 ISSN 1074-5521

Introduction

The renin–angiotensin system (RAS) is widely accepted as a major regulator of cardiovascular and renal function, and plays a major role in water and salt homeostasis, as well as blood pressure control. Its implication in various pathological states has been demonstrated by the efficacy of RAS blockers in conditions such as hypertension [1], cardiac failure [2] and left ventricular failure following myocardial infarction [3]. In addition, blockers of the RAS system are established drugs for renal protection [4,5]. The aspartic proteinase renin exclusively cleaves the peptide bond between Leu10 and Val11 in human angiotensinogen to form angiotensin I (Ang I), which is then further converted by angiotensin I converting enzyme (ACE) to the biologically active vasopressor octapeptide hormone Ang II. ACE can be bypassed by the serine proteinase chymase [6] and degrades other pharmacologically active peptides such as bradykinin. Chymase was recently shown to be the major Ang-II-forming enzyme in human heart tissue [7]. Ang II is known to act on two receptor subtypes, AT_1 and AT_2. With the recently discovered novel systems Ang 1–7 [8] and Ang 3–8 peptides [9] and their specific receptors AT_3 and AT_4 with largely unknown function, the RAS becomes even more complex. Because chymase is not inhibited by ACE inhibitors and, moreover, the available AT receptor antagonists only block receptors of the AT_1 subtype, the only totally effective control of the RAS system is provided through the inhibition of the rate-limiting and highly selective enzyme renin. The expected improved efficacy of a renin blocker in the tissue systems of the heart and kidneys will potentially improve the prevention and treatment of end organ damage in these tissues.

A significant number of peptidomimetic inhibitors of human renin designed as stable transition-state analogues of the scissile amide bond in human angiotensinogen have been developed that reached clinical phase II trials [10–12]. Despite the established clinical efficacy of several of the inhibitors, almost all development compounds were abandoned for reasons of limited oral bioavailability and/or excessive production costs [13]. It seemed necessary, therefore, to identify structural classes of nonpeptidomimetic renin inhibitors that would satisfy the necessary criteria for being more promising drug candidates. High-throughput screening of the Roche compound library identified a simple 3,4-disubstituted piperidine lead compound (**Ia**; Figure 1). The systematic optimisation of this structural class led to piperidine derivatives that have affinities for renin in the picomolar range [14].

Figure 1

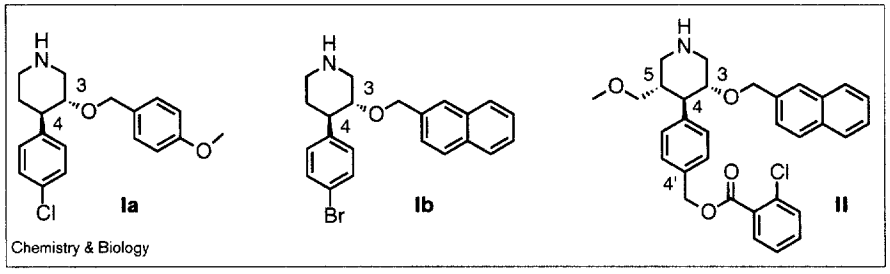

Chemical structures of the 4-halophenyl-piperidine compounds **Ia**, **Ib** and the 3,4,5-trisubstituted piperidine derivative **II**, which inhibit recombinant human renin with IC_{50} values of 26 μM (**Ia**), 5 μM (**Ib**) and 2 nM (**II**).

Understanding the enzyme inhibition at the structural level greatly aided the efficient optimisation of this class of inhibitors, with respect to specificity and affinity for renin. On the basis of the crystal structures of human recombinant renin complexed with two members of this structural class, a 3,4-disubstituted and a 3,4,5-trisubstituted piperidine derivative (**Ib** and **II**; Figure 1), respectively, a novel concept for renin inhibition is presented. The conformation of the inhibitors and their interactions with the enzyme will be described and an unexpected induced-fit adaptation of the enzyme active site will be discussed.

Results and discussion

The piperidine compound **Ib**, *trans* (3*R*,4*R*)-2-naphthylmethoxy-4-(4-bromophenyl)-piperidine, inhibits human recombinant renin in the low micromolar range (IC_{50} = 5 μM). Structural information about the binding mode of this new class of nonpeptidomimetic renin inhibitors was obtained by soaking cubic crystals of the glycosylated apoenzyme [15] with **Ib**. Using the protein structure observed in the complex with remikiren [16] as a model yielded clear molecular-replacement parameters for the two molecules in the asymmetric unit (see the Materials and methods section). Despite the moderate resolution of 3.65 Å, a subsequent F_o–F_c difference map showed significant extra density in the active site of one of the two enzyme molecules present in the asymmetric unit. The strongest part of the difference density extended from the two essential catalytic aspartates, Asp32 and Asp215 (pepsin numbering scheme is used throughout the text), along the amino-terminal side of the substrate cleft. Interpretation of the electron density proved difficult, and in our first attempts we assumed that the structure of the active site had remained the same as observed in the complex with remikiren (Figure 2). The best fit to the difference density was obtained by having the bromophenyl substituent pointing towards the S3 pocket. The inhibitor's piperidine nitrogen could be positioned near the two catalytic carboxylates but not close enough to make direct hydrogen bonds. With this very tentative interpretation, extensive structural variations in the 3-, 4- and 5-substituent positions appeared possible and, indeed, some highly potent compounds such as the 3,4,5-trisubstituted piperidine derivative **II** were obtained. The emerging structure–activity relationship soon became inconsistent with this binding hypothesis, however. Revision of the binding hypothesis, based on induced-fit adaptations around the enzyme's active site, became obvious once the complex with the 3,4,5-trisubstituted piperidine derivative (**II**; IC_{50} = 2 nM) was crystallised in a tetragonal, better-diffracting crystal form.

Figure 2

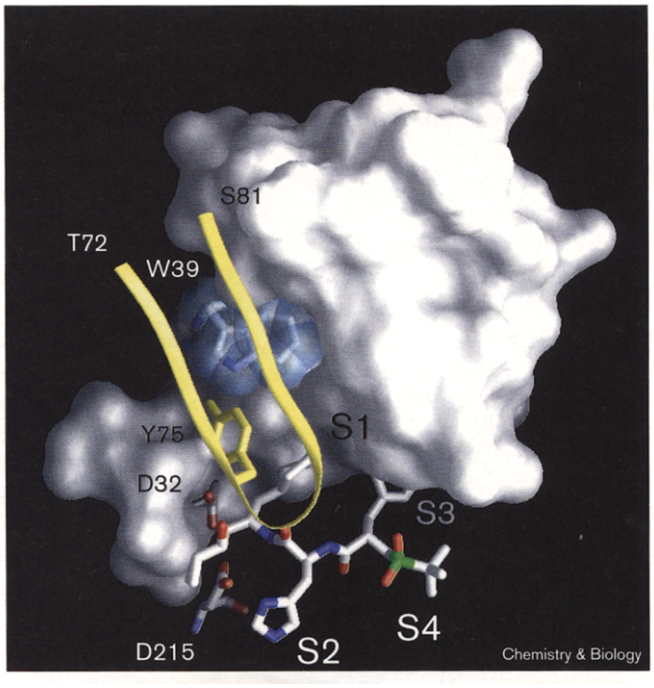

Molecular surface of the S1- and S3-binding pockets [34] in a complex of human recombinant renin with the peptidomimetic inhibitor remikiren. The sidechain of Trp39 is shown in light blue. The two catalytic residues, Asp32 and Asp215, are indicated. The trace of the flap region ranging from residue Thr72–Ser81 is indicated in yellow, as is the sidechain of Tyr75. The S3-binding pocket is located on the rear side of the protein. This and the following surfaces were generated and displayed using the program GRASP [35]. For clarity only the fragments Ile20, Lys28–Glu31, Thr33–Ser36, Val40–Ser42, Cys45–Phe46 and Glu103–Gly122 have been taken into account, and single-letter amino-acid code is used.

Figure 3

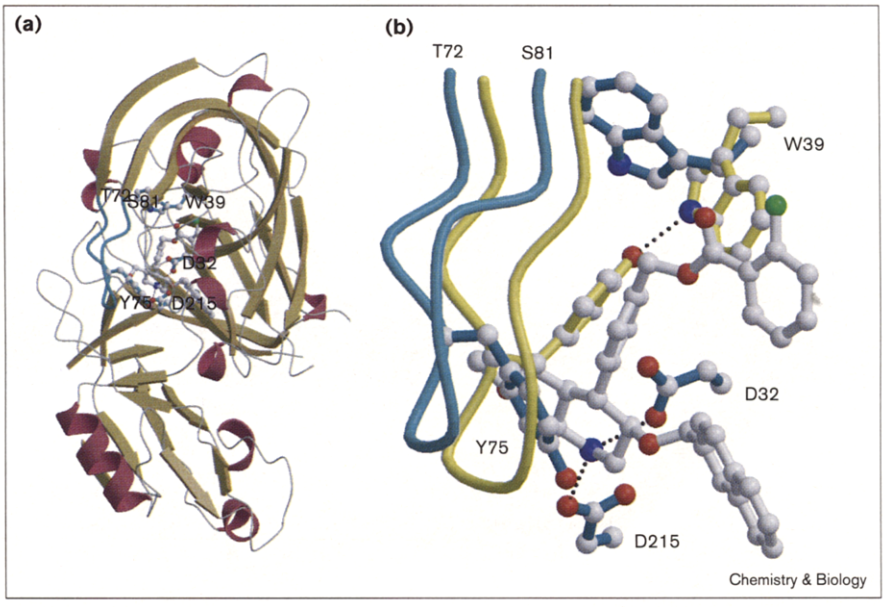

trans,trans-(3*R*,4*R*,5*S*)-4-[5-Methoxymethyl-3-(naphthalen-2-ylmethoxy)-piperidin-4-yl]-benzyl 2-chloro-benzoate **II** binding to human recombinant renin. The inhibitor in the active site is shown in ball-and-stick representation in white. **(a)** In the overall view, β strands are represented as arrows and α helices as ribbons. The flap region ranging from residue Thr72–Ser81 is light blue. Catalytic residues Asp32 and Asp215 and the sidechains of Trp39 and Tyr75 are shown. **(b)** The close-up view indicates the structural differences between the active site as observed in a complex with the peptidomimetic inhibitor remikiren [16] (yellow) and the piperidine derivative **II** (light blue). Hydrogen bonds are represented by dotted lines. The figure was produced using the programs MOLSCRIPT [36] and RASTER3D [37].

Structure determination of the complex of renin with compound **II** at 2.9 Å resolution permitted an unambiguous interpretation of the binding mode of this potent inhibitor and revealed some dramatic structural changes in the protein structure. In the refined structure, the protonated nitrogen of the piperidine moiety is positioned between the two catalytic aspartates, Asp32 and Asp215, such that it forms two strong hydrogen bonds with the enzyme. The lipophilic 2-naphthyl-methoxy substituent at position 3 occupies the large hydrophobic and contiguous subsites S1 and S3, which accommodate the P1 cyclohexyl and P3 phenyl sidechains of the peptidomimetic inhibitors CGP 38'560 [17] and remikiren [16], respectively. This nonpeptidomimetic inhibitor, therefore, lacks the P2 and the P4 portions, as well as the backbone of classical transition-state mimics. Given the orientation of the piperidine ring between the two catalytic aspartate residues, the large substituent at position 4 can only be accommodated by inducing major conformational changes in the protein structure compared with what is seen in the apoenzyme structure and in all the known structures of enzyme–transition-state analogue complexes [16–20]. The phenyl moiety at position 4 points towards the former carboxy-terminal boundary of the S1 pocket (Figures 2 and 3) occupied by the flap (Thr72–Ser81) or, more specifically, by the sidechain of Tyr75 in the closed structures. To make room for this part of the inhibitor, the flap shifts into a more open conformation and the sidechain of Tyr75 swings outwards through an approximately –120° χ1 rotation. This opening and rearrangement of the flap is not sufficient to provide space for the o-chlorobenzoyloxymethyl moiety of the 4-substituent (4′ substituent), however. This is achieved by additional displacement of the Trp39 sidechain, which flips into a new position. Closer examination of the structure of the residues shaping the cavity burying either the Trp39 sidechain or the 4′ substituent reveals some interesting aspects. In the complex with remikiren, the indole nitrogen of Trp39 makes a hydrogen bond with the phenolic OH functional group of Tyr75, but the indole sidechain is otherwise buried in a hydrophobic environment provided by the conserved residues Val40, Pro41, Val80, Val104, Met107, Phe112, Asp118, Gly119 and Val120. In the complex with compound **II**, the cavity formerly occupied by the indole ring of Trp39 is entirely filled with the o-chlorophenyl moiety of the inhibitor. The somewhat different shape of the inhibitor moiety is very well accommodated through a number of small changes in mainchain and sidechain conformations of the cavity-forming residues. The only unfavourable consequence of the burying of the 4′-substituent is that the carbonyl oxygen of the ester moiety has no hydrogen-bonding partner. In its new position, essentially reached by a –120° χ1 and a 180° χ2 rotation, the Trp39 sidechain is again almost completely buried in a hydrophobic environment, its benzene ring being covered by lipophilic sidechains of the flap region (mainly the sidechains of Leu71, Leu73 and Val80). The only solvent-accessible part of Trp39 is the indole nitrogen. The equatorial methoxymethyl function at position 5 points towards the flap region and just about touches one edge of the Tyr75 sidechain but does not contribute significantly to the high affinity of this inhibitor.

It was reasonable to believe that the related but lower-affinity compound **Ib** would bind to renin using a similar

Figure 4

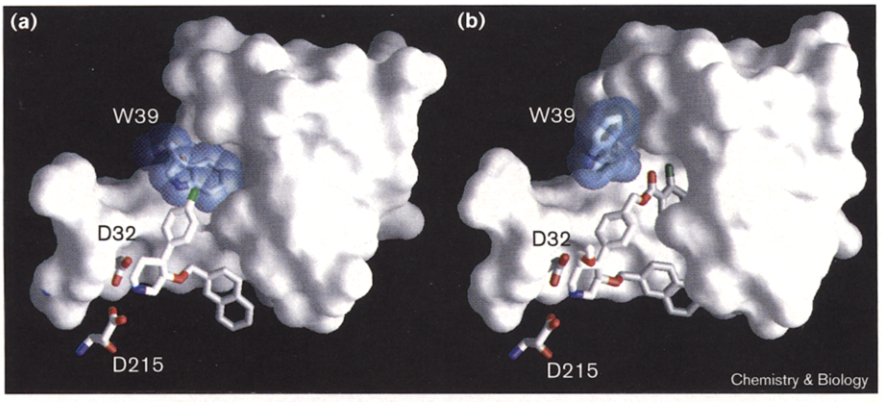

Comparison of the molecular surfaces of the binding pockets in a complex of human recombinant renin with the piperidine compounds **(a) Ib** and **(b) II**. The sidechain of Trp39 is light blue. The two catalytic residues Asp32 and Asp215 are indicated. The orientation is approximately orthogonal to that of Figure 3. For clarity, the flap region is not shown.

binding mode to compound **II**. Indeed, re-examination of the difference density obtained from the renin–**Ib** complex shows it to be very compatible with such a binding mode; the flap of the enzyme opens, which leads to the loss of the intramolecular hydrogen bond between the phenolic OH functional group of Tyr75 and the ring nitrogen of Trp39. There is no evidence, however, that the sidechain of Trp39 flips out of its pocket (Figure 4a), a structural alteration that is observed for the extended substituent at the 4′ position of compound **II** (Figure 4b). The introduction of the o-chlorobenzoyloxymethyl substituent (at the 4′ position of compound **II**) leads to an increase in renin binding affinity by more than 250-fold. The interface area between the essentially solvent-inaccessible 4′-substituent and the enzyme is about 130 Å^2, which translates into about 4 kcal/mol binding energy, using typical values for hydrophobic interactions [21]. The fact that this is not far from the gain in affinity suggests that the induced conformational change, the further opening of the flap and the relocation of Trp39, is not too costly in terms of energy. The observed IC_{50} of 2 nM for compound II is in the range obtained with highly potent peptidomimetic inhibitors such as remikiren [16] and CGP 38'560 [17].

Dramatic alteration of the shape of a binding site upon ligand binding is well documented for antibodies [22–25]. In the case of progesterone binding to its monoclonal anti-progesterone antibody DB3, the indole sidechain of TrpH100 adopts two different conformations, interconverting between 'open' and 'closed' forms of the antibody-combining site. The indole appears to be acting as an antibody-derived surrogate for its own hydrophobic pocket [26]. The observed induced-fit adaptations of the renin active site suggest that aspartic proteinase active sites have latent conformational flexibility. The main-chain and sidechain alterations of the binding pockets obviously depend on the substitution pattern of the piperidine moiety and provide sufficient variability for improved selectivity. Recently, the first crystal structure of plasmepsin II, a protein from *Plasmodium falciparum*, was reported [27]. The enzyme belongs to a group of two homologous monomeric aspartic proteinases, plasmepsin I and II, that are essential components of the hemoglobin-degradation pathway of *P. falciparum*. Indeed, compound II inhibits plasmepsin I and II with IC_{50} values of about 1 μM (data not shown). These observations suggest that the induced-fit adaptations observed for renin are of a more general nature and might therefore represent a novel paradigm for the inhibition of monomeric aspartic proteinases.

Significance

Renin, an aspartic proteinase, plays an important physiological role in the regulation of blood pressure. It catalyses the first and rate-limiting step in the conversion of angiotensinogen to the hormone angiotensin II. Although many potent peptidomimetic inhibitors of renin have been synthesised, none have been developed into antihypertensive drugs. A novel class of nonpeptidomimetic inhibitors have been developed here. Structural analysis reveals that binding of these piperidine-derived compounds to renin requires major conformational changes in the enzyme active site. Major changes to the shape of binding sites upon ligand binding have been well documented in antibodies [22–25]. The observed induced-fit adaptations of the renin active site suggest that aspartic proteinase active sites have latent conformational flexibility. This would be in agreement with the observation that piperidine derivatives also inhibit plasmepsin I and II from *Plasmodium falciparum*. The induced-fit adaptations observed for renin therefore could be of a more general nature, and might represent a novel paradigm for the inhibition of monomeric aspartic proteinases. The fact that the piperidine moiety can be an efficient binding partner for the catalytic aspartic acid residues suggests it could be used as a central template for aspartic proteinase inhibitors.

Materials and methods

Recombinant human renin, produced in chinese hamster ovary (CHO) cells [16], was crystallised in the apo form (form I) as described by Lim *et al.* [15] and in the inhibited form (form II) as described by Rahuel *et al.* [17]. Form I crystals belong to the cubic space group $P2_13$ with cell dimensions a = b = c = 143.3 Å, and crystal form II has space group $P4_12_12$ with a = b = 93.1 Å, c = 111.2 Å. For soaking experiments, native crystals were placed in 400 µl stabilising solution, containing a molar excess of the inhibitor **Ib**. A complex of renin with compound **II** was prepared by adsorbing purified apo-renin onto an affinity column to which a weak peptidomimetic renin inhibitor had been covalently coupled. Bound renin was then eluted with a solution of compound **II**. Excess inhibitor was removed by diafiltration. This approach was necessary due to its limited solubility in aqueous buffers. Diffraction data for both crystal forms were recorded at room temperature on a Siemens/Nicolet area detector installed on an Elliot GX-21 rotating anode generator operated at 40 kV, 80 mA and equipped with a graphite monochromator. Data processing was performed with the XDS software [28] and data reduction with the CCP4 suite [29]. The data collection statistics for crystal forms I and II were as follows: number of measurements, 37608/57052; number of independent reflections, 11033/10998; completeness (%), 98.3 (to 3.65 Å)/97.1 (to 2.9 Å); R_{merge} = 0.045/0.069 ($R_{merge} = \Sigma|I(k)-\langle I\rangle|/\Sigma I(k)$, where I(k) and ⟨I⟩ are the intensity values for individual measurements and of the corresponding mean values; the summation is over all measurements). The structure of the binary complex with the trans (3*R*,4*R*)-2-naphthylmethoxy-4-(4-bromophenyl)-piperidine [**Ib**] was solved by molecular replacement using MERLOT software [30] using the refined coordinates of the recombinant human enzyme as determined in the binary complex with remikiren [16]. The results obtained for the rotation and translation searches correspond to those published by Dhanaraj *et al.* [20]. Rigid body refinement converged to an R-factor of 21.4%. An F_c–F_c difference electron density map (where F_o and F_c are the observed and calculated structure factors, respectively) was calculated using the phases of the refined coordinates. Rigid body refinement of the binary complex with remikiren followed by positional and restrained B-value refinement performed with X-PLOR [31] converged to a final R-factor ($R = \Sigma||F_o|-|F_c||/\Sigma|F_o|$) of 16.0% for 10980 reflections at 2.9 Å for the data of the binary complex with compound II. Parameters for ideal stereochemistry were used as described by Engh and Huber [32], manual rebuilding was performed using the in-house graphics program MOLOC [33]. The root-mean-square deviation from target values for bonds and angles is 0.018 Å and 2.22°, respectively.

Acknowledgements

We are grateful to M. Stihle for excellent technical assistance and thank D.W. Banner for helpful discussions and carefully reading the manuscript.

References

1. Waeber, B., Nussberger, J. & Brunner, H.R. (1986). The renin-angiotensin system: role in experimental and human hypertension. In *Handbook of Hypertension, Vol. 8: Pathophysiology of Hypertension – Regulatory Mechanisms* (Zanchetti, A. & Tarazi, R.C., eds), pp. 489-519, Elsevier Science Publishing Co., Amsterdam.
2. Fouad-Tarazi, F., Bumbus, M., Khosla, M. & Healy, B. (1988). The renin-angiotensin system and treatment of heart failure. *Am. J. Med.* **84** (suppl 3A), 83-86.
3. Pfeffer, M.A., *et al.*, & Hawkins, C.M. (1992). Effect of captopril on mortality and morbidity in patients with left ventricular dysfunction after myocardial infarction. *N. Engl. J. Med.* **327**, 669-677.
4. Breyer, J.A., Hunsicker, L.J., Bain, R.P. & Lewis, E.J. (1994). ACE inhibition in diabetic nephropathy. *Kidney Int.*, S156-S160.
5. Maschio, G. (1996). ACEI in the progressive renal insufficiency group (various renal diseases). *N. Engl. J. Med.* **334**, 939-945.
6. Urata, H., Healy, B., Steweart, R.W., Bumpus, F.M. & Husain, A. (1990). Angiotensin II-forming pathways in normal and failing human hearts. *Circ. Res.* **66**, 883.
7. Wolny, A., *et al.*, & Fischli, W. (1997). Functional and biochemical analysis of angiotensin II-forming pathways in the human heart. *Circ. Res.* **80**, 219-227.
8. DelliPizzi, A.M., Hilchey, S.D. & Bell-Quilley, C.P. (1994). Natriuretic action of Angio(1-7). *Br. J. Pharmacol.* **111**, 1-3.
9. Swanson, G.N., *et al.*, & Harding, J.W. (1993). Discovery of a distinct binding site for angio(3-8), a putative AT4 receptor. *Regul. Pept.* **40**, 409-419.
10. Kleinert, H.D. (1994). Recent developments in renin inhibitors. *Exp. Opin. Invest. Drugs* **3**, 1087-1104.
11. Raddatz, P. (1994). Recent developments in renin inhibitors: part I. *Exp. Opin. Ther. Patents* **4**, 489-504.
12. Raddatz, P. (1994). Recent developments in renin inhibitors: part II. *Exp. Opin. Ther. Patents* **4**, 1347-1359.
13. Kleinert, H.D. (1995). Renin inhibition. *Cardiovasc. Drug Ther.* **9**, 645-655.
14. Binggeli, A., *et al.*, & Wostl, W. (1996). New piperidine derivatives as renin-inhibitors. *World (PCT) Patent WO* 9709311-A1.
15. Lim, L.W., Stegeman, R.A., Leimgruber, N.K., Gierse, J.K. & Abdel-Meguid, S.S. (1989). Preliminary crystallographic study of glycosylated recombinant human renin. *J. Mol. Biol.* **210**, 239-240.
16. Mathews, S., *et al.*, & Fischli, W. (1996). Recombinant human renin produced in different expression systems: biochemical properties and 3D structure. *Protein Exp. Purif.* **7**, 81-91.
17. Rahuel, J., Priestle, J.P., Grütter, M.G. (1991). The crystal structures of recombinant glycosylated human renin alone and in complex with a transition state analog inhibitor. *J. Struct. Biol.* **107**, 227-236.
18. Sielecki, A.R., *et al.*, & James, M.N. (1989). Structure of recombinant human renin, a target for cardiovascular-active drugs, at 2.5 Å resolution. *Science* **243**, 1346-1351.
19. Badasso, M., *et al.*, & Szelke, M. (1992). Crystallization and preliminary X-ray analysis of complexes of peptide inhibitors with human recombinant and mouse submandibular renins. *J. Mol. Biol.* **223**, 447-453.
20. Dhanaraj V., *et al.*, & Hoover, D.J. (1992). X-ray analyses of peptide-inhibitor complexes define the structural basis of specificity for human and mouse renins. *Nature* **357**, 466-472.
21. Sharp, K.A., Nicholls, A., Friedman, R. & Honig, B. (1991). Extracting hydrophobic free energies from experimental data: relationship to protein folding and theoretical models. *Biochemistry* **30**, 9686-9697.
22. Stanfield, R.L., Fieser, T.M., Lerner, R.A. & Wilson, I.A. (1990). Crystal structures of an antibody to a peptide and its complex with peptide antigen at 2.8 Å resolution. *Science* **248**, 712-719.
23. Bhat, T.N., Bentley, G.A., Fischmann, T.O., Boulot, G. & Poljak, R.J. (1990). Small rearrangements in structures of Fv and Fab fragments of antibody D1.3 on antigen binding. *Nature* **347**, 483-485.
24. Herron, J.N., *et al.*, & Edmundson, A.B. (1991). An autoantibody to single-stranded DNA: comparison of the three-dimensional structures of the unliganded Fab and a deoxynucleotide-Fab complex. *Proteins* **11**, 159-175.
25. Rini, J.M., Schulze-Gahmen, U. & Wilson, I.A. (1992). Structural evidence for induced fit as a mechanism for antibody–antigen recognition. *Science* **255**, 959-965.
26. Arevalo, J.H., Stura, E.A., Taussig, M.J. & Wilson, I.A. (1993). Three-dimensional structure of an anti-steroid Fab' and progesterone-Fab' complex. *J. Mol. Biol.* **231**, 103-118.
27. Silva, A.M., *et al.*, & Erickson, J.W. (1996). Structure and inhibition of plasmepsin II, a hemoglobin-degrading enzyme from *Plasmodium falciparum*. *Proc. Natl Acad. Sci. USA* **93**, 10034-10039.
28. Kabsch, W. (1988). Evaluation of single-crystal X-ray diffraction data from a position-sensitive detector. *J. Appl. Crystallogr.* **21**, 916-924.
29. Collaborative Computational Project, Number 4. (1994). CCP4 Suite: programs for protein crystallography. *Acta Crystallogr. D* **50**, 760-763.
30. Fitzgerald, P.M.D. (1988). MERLOT, an integrated package of computer programs for the determination of crystal structures by molecular replacement. *J. Appl. Crystallogr.* **21**, 273-278.
31. Brünger, A.T. (1992). *X-PLOR Manual, version 3.1*, Yale University, New Haven, CT.
32. Engh, R. & Huber, R. (1991). Accurate bond and angle parameters for X-ray protein structure refinement. *Acta Crystallogr. A*, **47**, 392-400.
33. Gerber, P.R. (1992). Peptide mechanics: a force field for peptides and proteins working with entire residues as smallest units. *Biopolymers* **32**, 1003-1017.
34. Schechter, I., Berger, A. (1967). On the size of the active site in proteases. I. Papain. *Biochem. Biophys. Res. Commun.* **27**, 157-162.
35. Nicholls, A. & Honig, B. (1992). *GRASP: Graphical Representation and Analysis of Surface Properties*. Columbia University, New York.
36. Kraulis, P.J. (1991). MOLSCRIPT: a program to produce both detailed and schematic plots of protein structures. *J. Appl. Crystallogr.* **24**, 946-950.
37. Meritt, E.A. & Bacon, D.J. (1997). Raster3D: photorealistic molecular graphics. *Methods Enzymol.* **277**, 505-524.